Electronic Supplementary Material (ESI) for Journal of Materials Chemistry C.

Ferroelectricity of Alkylamide-substituted Triptycene Derivatives

Ryohei Mizoue,[a] *Takashi Takeda,*[a, b, c] *Shun Dekura,*[a, b] *Mikiya Kato,*[d, e] *Tomoya Fukui,*[d, e] *Yoshiaki Shoji,*[d, e] *Takanori Fukushima,*[d, e, f] *Saya Yamane,*[g] *Yasutaka Suzuki,*[g] *Jun Kawamata,*[g] *and Tomoyuki Akutagawa* [a, b]*

[a] Graduate School of Engineering, Tohoku University, Sendai 980-8579, Japan, [b] Institute of Multidisciplinary Research for Advanced Materials (IMRAM), Tohoku University, 2-1-1 Katahira, Aoba-ku, Sendai 980-8577, Japan, [c] Faculty of Science, Shinshu University, 3-1-1 Asahi, Matsumoto 390-8621, Japan, [d] Laboratory for Chemistry and Life Science, Institute of Innovative Research, Tokyo Institute of Technology, Yokohama 226-8503, Japan, and [e] School of Materials and Chemical Technology, Tokyo Institute of Technology, Yokohama 226-8503, Japan. [f] Living Systems Materialogy (LiSM) Research Group, International Research Frontiers Initiative (IRFI), Tokyo Institute of Technology, 4259 Nagatsuta, Midori-ku, Yokohama 226-8503, Japan. [g] Graduate School of Sciences and Technology for Innovation, Yamaguchi University, 1677-1 Yoshida, Yamaguchi, Yamaguchi, 753-8512, Japan.

Phone: +81-22-217-5653

Fax: +81-22-217-5655

E-mail akutagawa@tohoku.ac.jp

Contents

Experimental Section

General. High-resolution APCI-TOF mass spectrometry measurements were performed on a Bruker model microTOF II mass spectrometer equipped with an atmospheric pressure chemical ionization (APCI) probe. IR spectra (400–4000 cm^{-1}) on KBr pellets were measured using a Thermo Fisher Scientific Nicolet 6700 FT-IR spectrophotometer. Elemental analyses were measured on a Microcoder JM10 (J Science Lab. Co. Ltd). Thermogravimetric (TG) analysis and differential scanning calorimetry (DSC) were conducted using a Rigaku Thermo plus TG8120 thermal analysis station and a Mettler DSC1-T unit with an Al_2O_3 reference at a heating and cooling rate of 5 K min^{-1} under N_2-flow. Temperature-dependent powder X-ray diffraction patterns (PXRD) were obtained using a Rigaku Rint-Ultima diffractometer with Cu Kα radiation at λ=1.54187Å within the temperature range of 298−498 K. *T*-dependent dielectric constants were determined using the two-probe AC impedance method from 100 Hz to 1 MHz (Hewlett-Packard, HP4194A) and the temperature controller of a Linkam LTS-350 system. Ferroelectric polarization–electric field hysteresis (*P*–*E*) curves were acquired using a commercially available ferroelectric tester (Precision LC, Radiant Technologies). Solid-state samples were fabricated on indium tin oxide (ITO) glass (SZ−A311P6N), which was sandwiched between the corresponding ITO glass to form a dielectric measurement cell with an average electrode gap of 5 μm.

Preparation of C14TATP. A solution of 1,8,13-tricarboxytriptycene[53] (200 mg, 513 μmol) in dry chloroform (50 mL) and $SOCl_2$ (15 mL) was refluxed for 24 h. The reaction mixture was evaporated to dryness under reduced pressure. The residue was dissolved in dry chloroform (30 mL), and then anhydrous triethylamine (350 μL, 2.50 mmol) was added, followed by and

tetradecylamine (400 mg, 3.50 mmol). The resulting mixture was stirred at 25 °C for 24 h. The white precipitate formed was collected by filtration and subsequently recrystallized from tetrahydrofuran (THF), affording **C14TATP** (133 mg) as a white powder in 27% yield. ^{1}H NMR (400 MHz, $CDCl_3$): δ = 7.42 (dd, 3H, *J* = 7.3, 0.9 Hz), 7.15 (dd, 3H, *J* = 7.8, 1.2 Hz), 7.03 (dd, 3H, *J* = 6.8, 7.8 Hz), 6.81 (s, 1H), 6.75 (t, 3H, *J* = 5.4 Hz), 5.48 (s, 1H), 3.53 (dt, 6H, *J* = 9.0, 6.0 Hz), 1.74 (quin, 6H, *J* = 7.0 Hz), 1.49-1.32 (m, 66H), 0.91 (t, 9H, *J* = 7.0 Hz). Elemental analysis. Calced. for $C_{65}H_{101}N_3O_3$, C, 80.28; H, 10.47; N, 4.32; Found: C, 79.98; H, 10.37; N, 4.36.

Preparation of C6TATP. A solution of 1,8,13-tricarboxytriptycene[53] (500 mg, 1.28 mmol) in dry chloroform (30 mL) $SOCl_2$ (30 mL) was refluxed for 24 h. The reaction mixture was evaporated to dryness under reduced pressure. The residue was dissolved in dry chloroform (30 ml), and then anhydrous triethylamine (600 μL, 4.34 mmol) was added, followed by and hexylamine (400 μL, 3.50 mmol). The resulting mixture was stirred at 25 °C for 24 h. A white precipitate formed was collected by filtration and subsequently recrystallized from methanol, affording **C6TATP** (71.8 mg) as a white powder in 9% yield. ^{1}H NMR (400 MHz, $CDCl_3$): δ = 7.42 (dd, 3H, *J* = 7.3, 0.9 Hz), 7.15 (dd, 3H, *J* = 7.8, 1.2 Hz), 7.03 (dd, 3H, *J* = 7.8, 6.8 Hz), 6.81 (s, 1H), 6.75 (t, 3H, *J* = 5.4 Hz), 5.48 (s, 1H), 3.53 (dt, 6H, *J* = 9.0, 6.0 Hz), 1.74 (quin, 6H, *J* = 7.0 Hz), 1.49-1.32 (m, 18H), 0.91 (t, 9H, *J* = 7.0 Hz). Elemental analysis. Calced. for $C_{41}H_{50}N_3O_3$: C, 77.44; H, 8.40; N, 6.61; Found: C, 77.15; H, 8.50; N, 6.67.

Preparation of 1,8-dicarboxytriptycene. Under nitrogen at 0 °C, a tetrahydrofuran (THF) solution of methylmagnesium chloride (3.0 M, 20 mL, 60 mmol) was added dropwise to a THF solution (300 mL) of a mixture of 1,8-dichlorotriptycene[54] (4.85 g, 15.0 mmol) and 1,3-bis(diphenylphosphino)propane nickel(II) dichloride (1.14 g, 2.10 mmol), and the mixture was heated at 80 °C and stirred at this temperature for 24 h. After allowed to cool to 25 °C, the

reaction mixture was poured into water and extracted with dichloromethane. The combined organic extract was washed with water and brine, dried over anhydrous $MgSO_4$, and evaporated to dryness under reduced pressure. The residue was subjected to column chromatography on SiO_2 (hexane), to allow the isolation of 1,8-dimethyltriptycene (4.02 g, 14.2 mmol). This product (3.50 g, 12.4 mmol) was dissolved in a mixture of pyridine (200 mL) and water (120 mL), and the solution was heated at 100 °C, to which $KMnO_4$ (78.3 g, 495 mmol) was added portionwise over 48 h. After allowed to cool to 25 °C, the resultant suspension was passed through a plug of Celite®. The residue was washed thoroughly with an aqueous solution of KOH (1.5 wt%, 100 mL), and the soluble part was combined with the filtrate obtained by the Celite®-filtration. The combined filtrate was partially evaporated under reduced pressure, where the amount of the solution was reduced to approximately 100 mL. The resultant solution was acidified with an aqueous solution of hydrochloric acid (1 M). The precipitate formed was collected by filtration, washed with water and methanol, and dried under reduced pressure to give 1,8-dicarboxytriptycene (4.04 g, 11.8 mmol) in 89 % yield. ^{1}H NMR (400 MHz, DMSO-d_6): δ (ppm) 13.0 (s, 2H), 7.77 (s, 1H), 7.64 (d, 2H, J = 7.8 Hz), 7.49–7.45 (m, 3H), 7.42–7.39 (m, 1H), 7.11 (dd, 2H, J = 7.8, 7.8 Hz), 7.05–7.02 (m, 2H), 5.81 (s, 1H). ACPI-TOF mass: calcd. for $C_{22}H_{13}O_4$ $[M–H]^–$; m/z = 341.0808; found: 341.0796.

Preparation of C14DATP. C14DATP (312 mg) was obtained in 49% yield from 1,8-dicarboxytriptycene (300 mg) by a procedure similar to that for **C14TATP** except that acetonitrile was used for recrystallization. ^{1}H NMR (400 MHz, CD_3CN): δ = 7.64 (br, 2H), 7.56 (dd, 2H, J = 7.3, 0.9 Hz), 7.47 (dd, 1H, J = 6.6, 1.5 Hz), 7.34 (dd, 1H, J = 6.8, 1.6 Hz), 7.24 (dd, 2H, J = 7.8, 1.2 Hz), 7.12 (dd, 2H, J = 7.8, 6.8 Hz), 7.09-7.01 (m, 2H), 6.57 (s, 1H), 5.70 (s, 1H), 3.52 (dt, 4H, J = 10.6, 6.9 Hz), 1.82-1.71 (m, 4H), 1.54-1.24 (m, 44H), 0.90 (t, 6H, J = 6.7 Hz).

Calced. for $C_{50}H_{72}N_2O_2$, C, 81.92; H, 9.90; N, 3.82; Found: C, 81.65; H, 10.15; N, 3.99.

Preparation of C6DATP. C6DATP (47.8 mg) was obtained in 11% yield from 1,8-dicarboxytriptycene (300 mg) by a procedure similar to that for **C6TATP** except that acetonitrile was used for recrystallization. ^{1}H NMR (400 MHz, CD_3CN): δ = 7.64 (br, 2H), 7.56 (dd, 2H, *J* = 7.3, 0.9 Hz), 7.47 (dd, 1H, *J* = 6.6, 1.5 Hz), 7.34 (dd, 1H, *J* = 6.8, 1.6 Hz), 7.24 (dd, 2H, *J* = 7.8, 1.2 Hz), 7.12 (dd, 2H, *J* = 7.8, 7.4 Hz), 7.09-7.01 (m, 2H), 6.57 (s, 1H), 5.70 (s, 1H), 3.52 (dt, 4H, *J* = 10.6, 6.9 Hz), 1.82-1.71 (m, 4H), 1.54-1.24 (m, 12H), 0.90 (t, 6H, *J* = 6.7 Hz). Calced. for $C_{34}H_{40}N_2O_2$, C, 80.28; H, 7.93; N, 5.51; Found: C, 79.98; H, 7.97; N, 5.48.

Crystal structure determination. The crystallographic data of **C6DATP** was collected using a Rigaku RAPID-II diffractometer equipped with a rotating anode, fitted with a multilayer confocal optic, using Cu Kα (λ = 1.54187 Å) radiation from a graphite monochromator. Structural refinements were performed using the full-matrix least-squares method on F^2. Calculations were performed using the Crystal Structure software packages.[55, 56] All parameters were refined using anisotropic temperature factors, except for those of the hydrogen atoms. The π-electron compounds substituted with alkylamide chains that form one-dimensional amide hydrogen bonds are commonly observed to form organogels and nanofibers, and difficulties are generally encountered in growing single crystals. The crystals reported here are the most highly crystalline single crystals. The data were collected at a temperature of 100 K to a maximum 2θ value of 136°. Exposure time was also tried from 30 to 120 seconds per frame, but since there was no significant change in the reflection peak at the wide-angle side, we used an exposure time of 30 second / frame, which minimizes background effects, and an omega-scan every 15.0° for a scan width range from 8 to 260.0°. A total of 60 oscillation images were collected. A sweep of data was done

using ω-scans from 80.0 to 260.0°in 15.00° step, at χ = 54.0° and ϕ = 0.0°. The exposure rate was 30.0 sec / frame. A second sweep was performed using ω scans from 80.0 to 260.0° in 15.00° step, at χ = 54.0° and ϕ = 90.0°. The exposure rate was 30.0 second / frame. Another sweep was performed using ω scans from 80.0 to 260.0° in 15.00° step, at χ = 54.0° and ϕ = 180.0°. The exposure rate was 30.0 second /frame. Another sweep was performed using ω scans from 80.0 to 260.0° in 15.00° step, at χ = 54.0° and ϕ = 270.0°. The exposure rate was 30.0 second /frame. Another sweep was performed using ω scans from 80.0 to 260.0° in 15.00° step, at χ = 0.0° and ϕ = 0.0°. The exposure rate was 30.0 second /frame. The crystal-to-detector distance was 127.40 mm. Readout was performed in the 0.100 mm pixel mode. $C_{41}H_{50}N_3O_3$, M = 576.63, $P2_1/c$ (#14), T = 100 K, a = 15.8016(13), b = 16.2173(13), c = 25.8540(10) Å, β = 100.628(7)°, V = 3603.0(5) $Å^3$, Z = 4, D_c = 1.172 g cm^{-3}, μ = 5.762 cm^{-1}, independent reflections 38467, reflection used 6489, R_{int} = 0.1985, R_1 = 0.0991, R_{all} = 0.2523, $R_w(F_2)$ = 0.2934, GOF = 0.885, and CCDC= 2295387.

Second harmonic generation (SHG) microscope. A femtosecond fiber laser oscillating at 1030 nm (Hamamatsu Photonics, BD1081) was used as the light source. A quarter-wavelength plate was used to generate circular polarization to avoid the polarization dependence of the crystal. The laser beam was scanned using a galvano mirror system (Hamamatsu Photonics, C10516). This scan was used to obtain two-dimensional microscopic images. Subsequently, the direction of the z-axis of the stage was moved to obtain a 3D microscopic image. A dichroic mirror (cutoff at 780 nm) was employed, and the reflected beam was focused on the sample using a ×20 objective with a numerical aperture of 0.45. The fluorescence from the sample was detected using a photomultiplier tube (Hamamatsu Photonics, H7421-40). To confirm the nonlinear process as

multi-photon absorption, we performed SHG microscope using a light source oscillating at 860 nm. In general, SHG is an efficient process compared to multi-photon processes and occurs in non-centrosymmetric crystals, is generated at a wavelength that is half the wavelength of the incident light. In other words, wavelengths of 515 nm (green light) and 430 nm (blue light) were observed when light sources oscillating at 1030 and 860 nm were used, respectively. However, the fluorescence remained blue regardless of the light source used. Therefore, the fluorescence was confirmed to be more dominant in this crystal than in SHG.

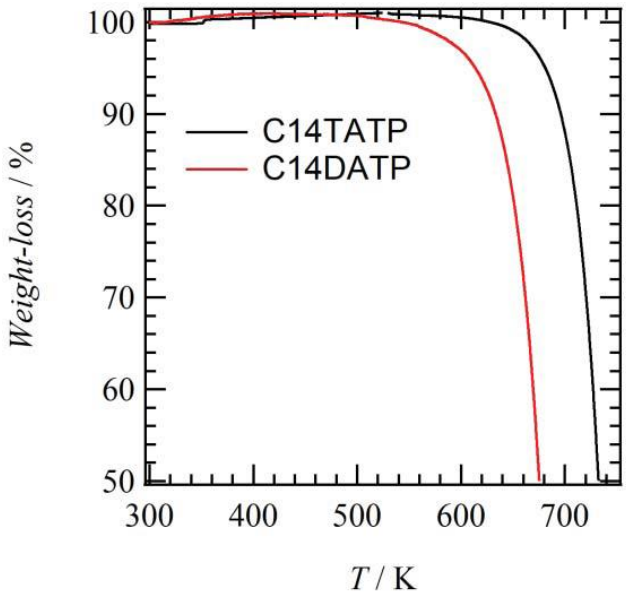

Figure S1. TG charts of **C14TATP** and **C14DATP**.

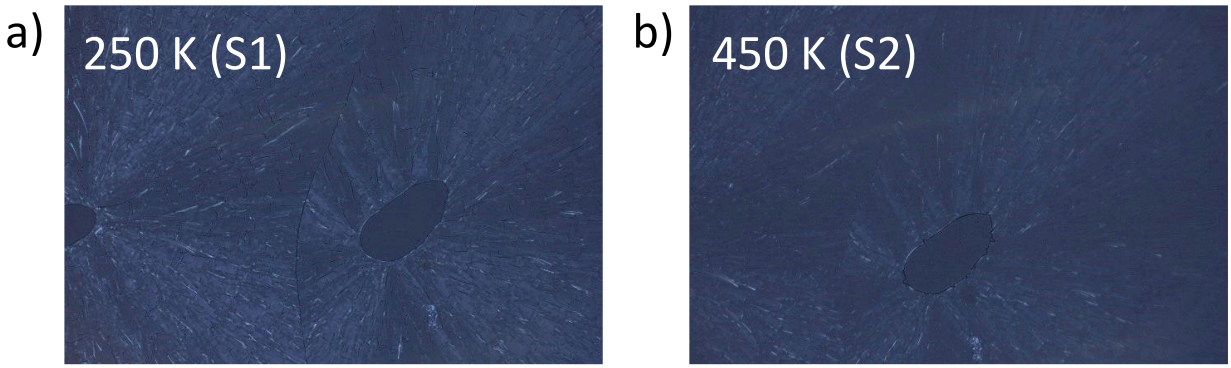

Figure S2. Temperature dependent POM images of **C14DATP** at 250 and 450 K.

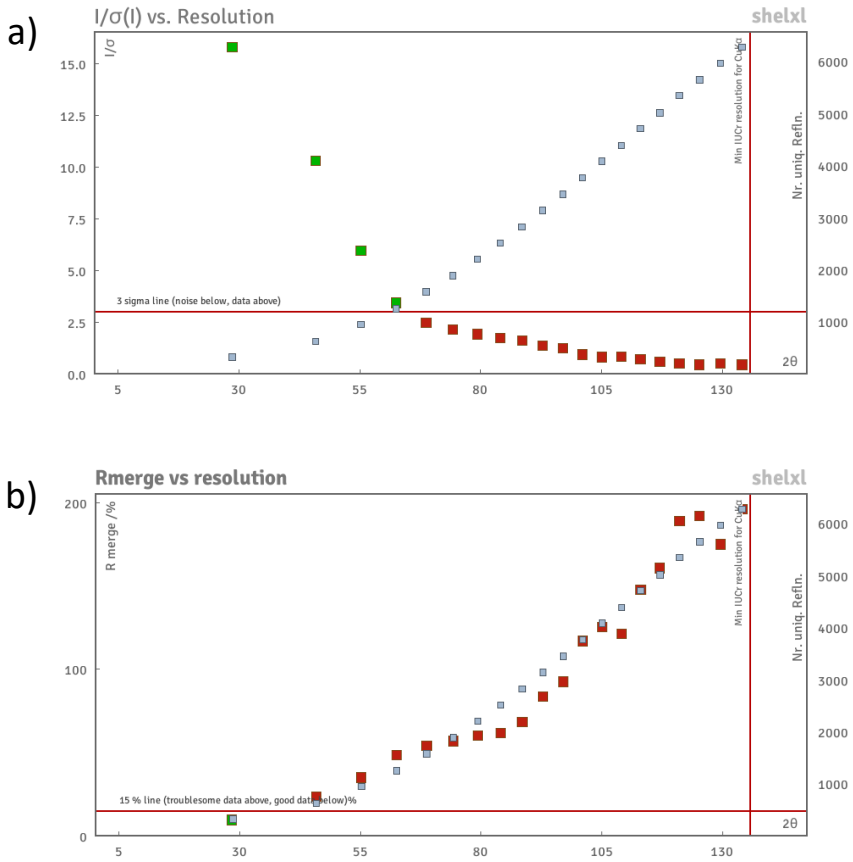

Figure S3. Resolution vs I / σ(I) and R-merge plots for structural analysis of **C6TATP** at 100 K.

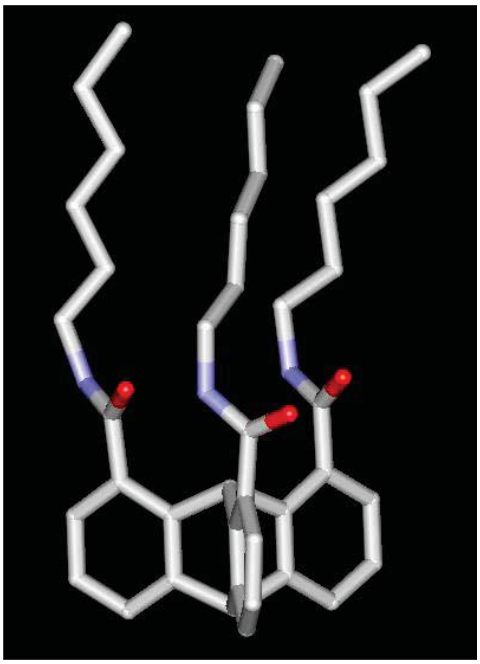

Figure S4. Molecular structure of **C6TATP** at 100 K.

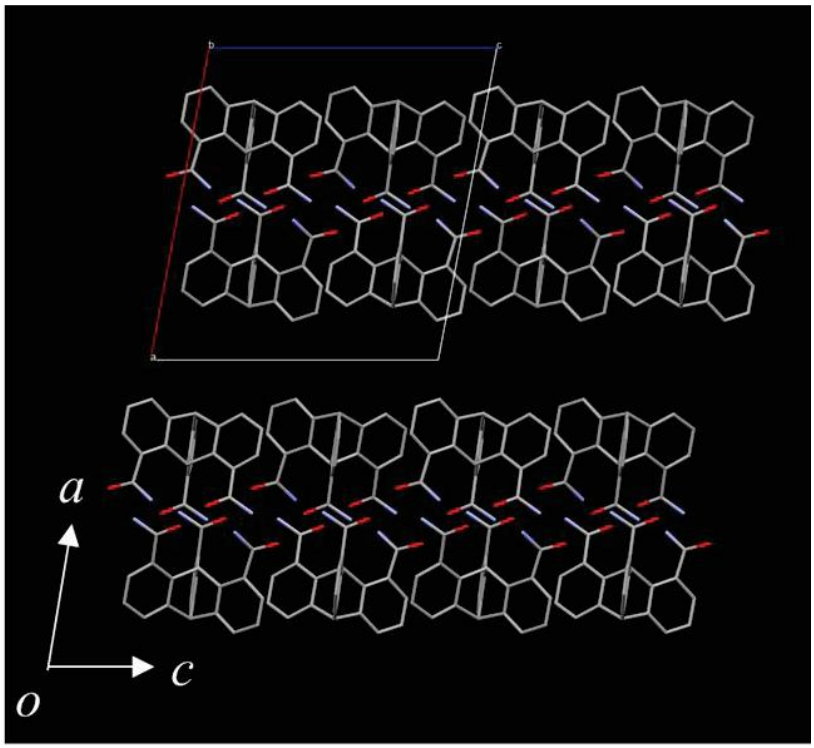

Figure S5. Unit cell of **C6TATP** at 100 K viewed along the *b*-axis. Alkyl chains were omitted to clarify hydrogen-bonding interaction.

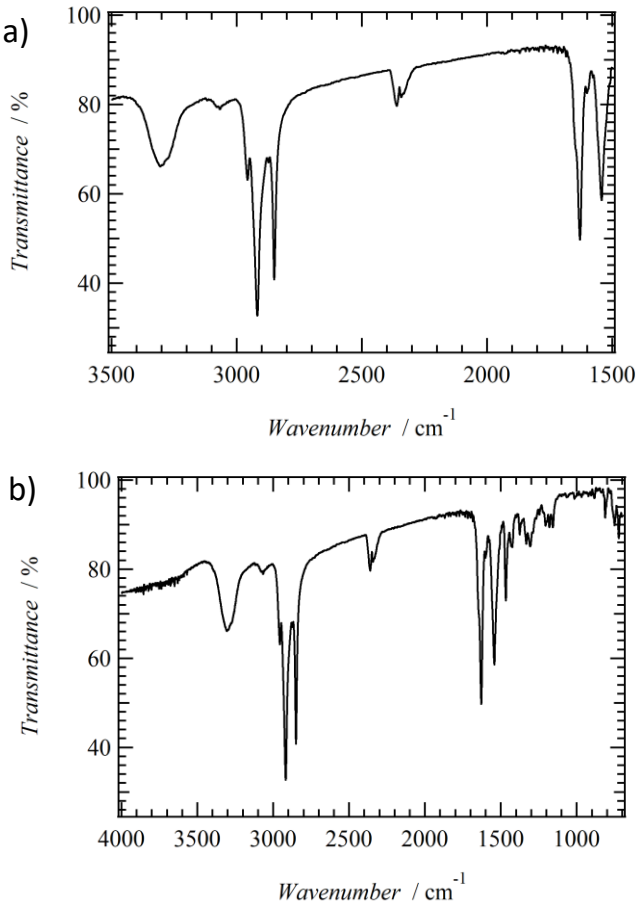

Figure S6. IR spectra of a) **C14TATP** and b) **C14DATP** on KBr pellets at 298 K.

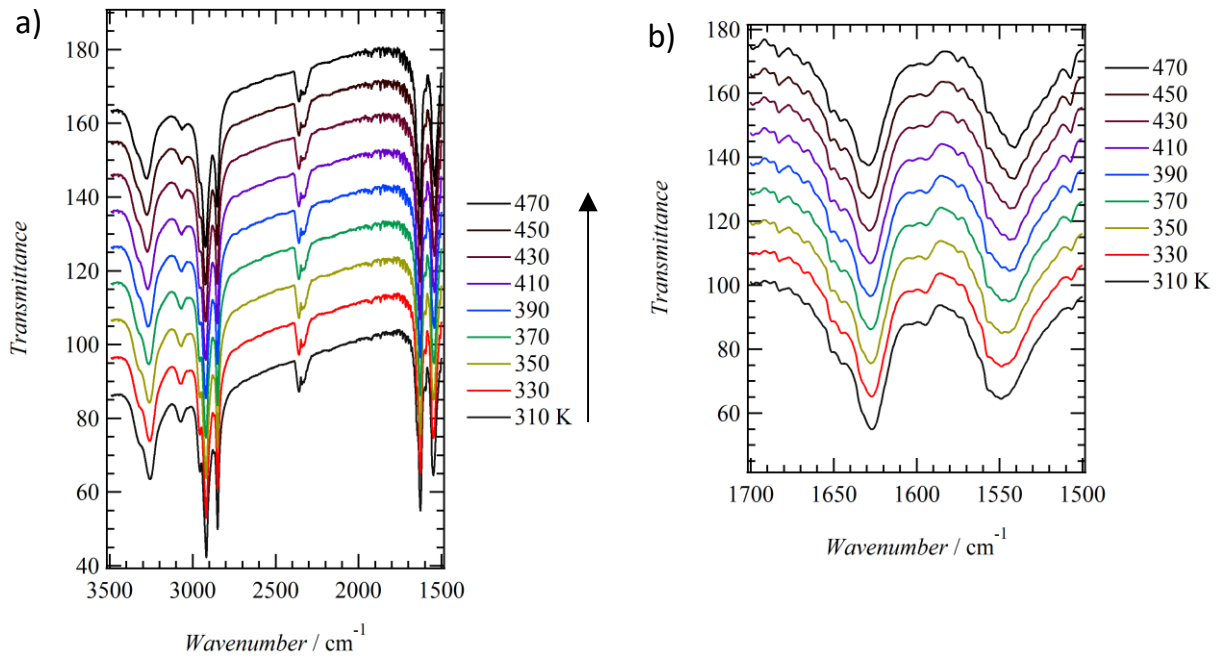

Figure S7. *T*-dependent IR spectra of **C14TATP** at energy range of a) 1500~3500 cm^{-1} and b) 1500~1700 cm^{-1}.

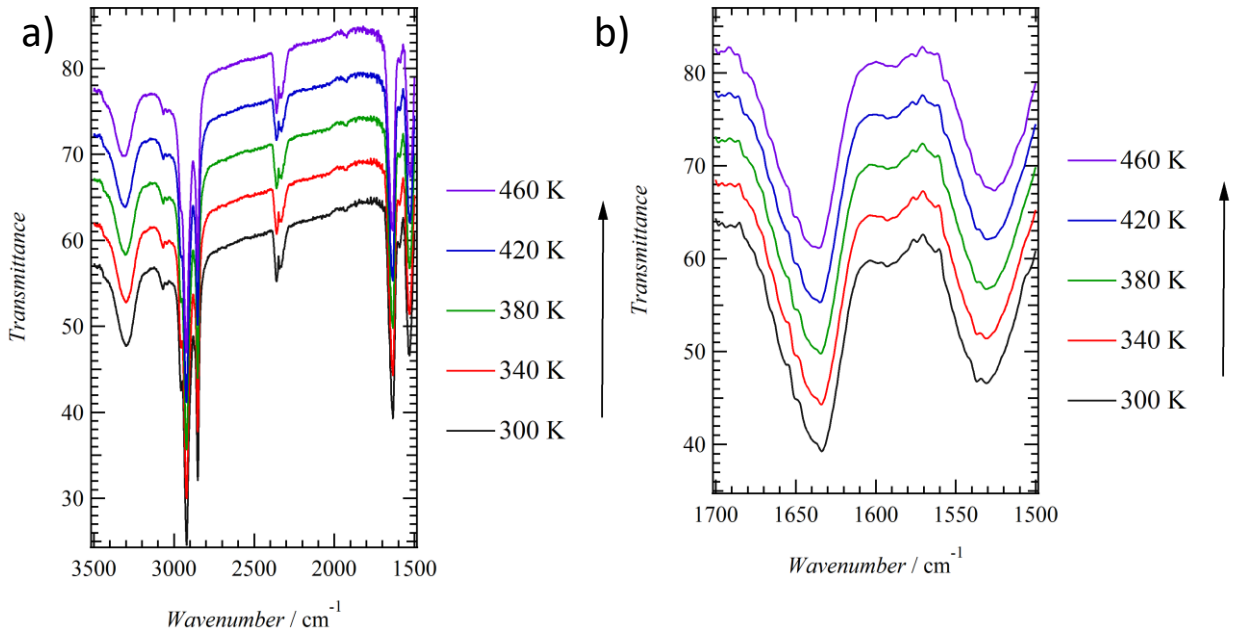

Figure S8. *T*-dependent IR spectra of **C14DATP** at energy range of a) 1500~3500 cm^{-1} and b) 1500~1700 cm^{-1}.

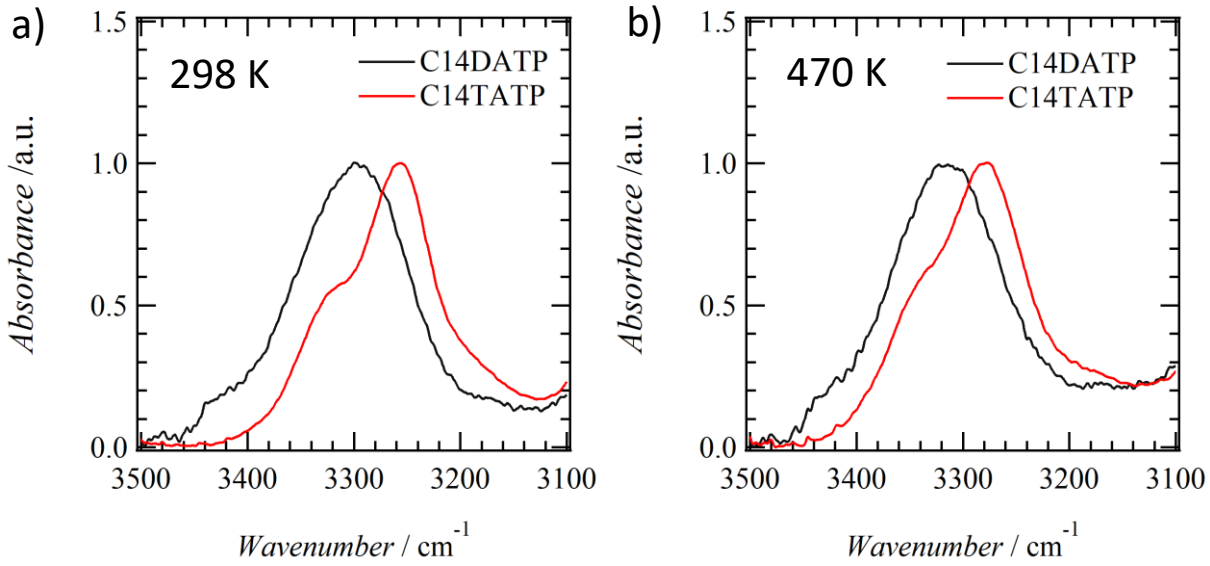

Figure S9. FWHM of N-H vibration bands on IR spectra at a) 298 and b) 470 K.

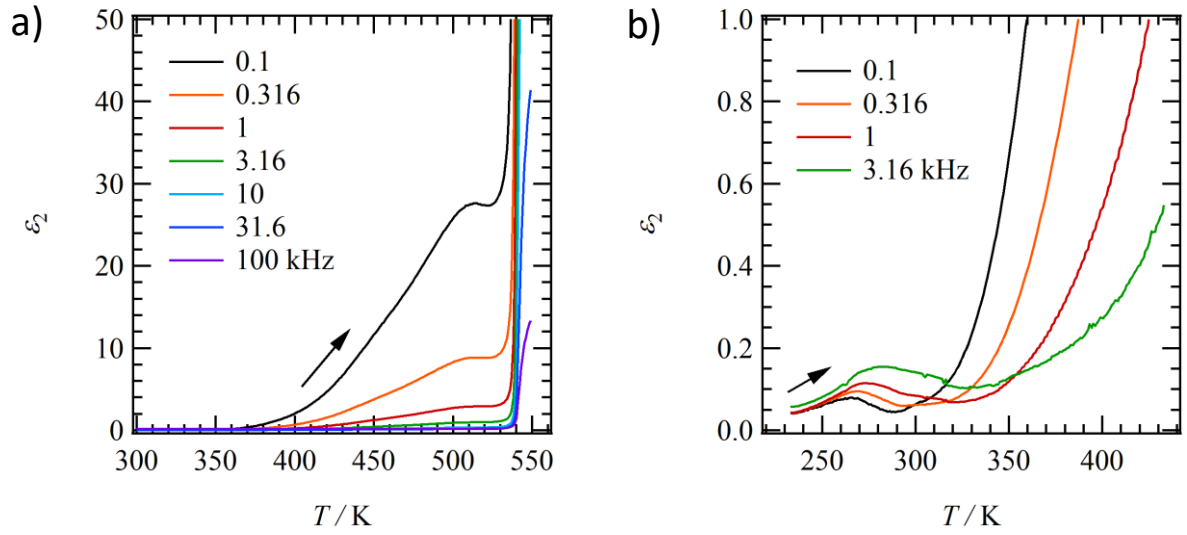

Figure S10. *T*- and *f*-dependent imaginary part dielectric constants ε_2 of a) **C14TATP** and b) **C14DATP** using the compressed pellets.

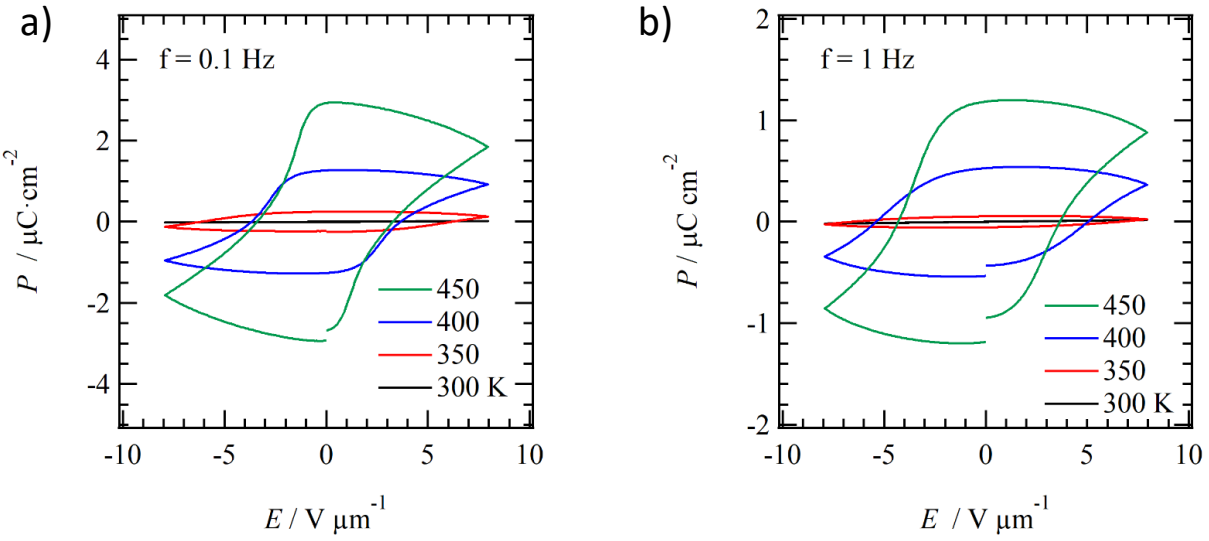

Figure S11. *T*-dependent *P*-*E* hysteresis curves of **C14TATP** at a) f = 0.1 Hz and b) f = 1.0 Hz.

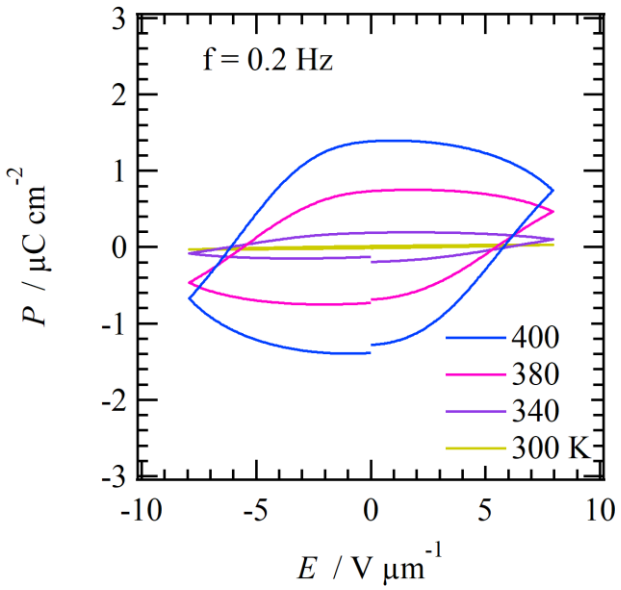

Figure S12. *T*-dependent *P*-*E* hysteresis curves of **C14DATP** at f = 0.2 Hz.

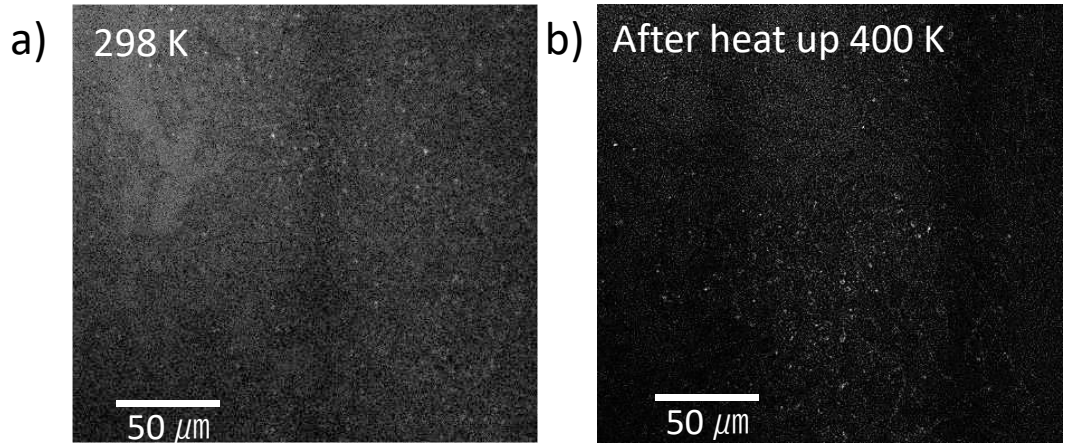

Figure S13. *T*-dependent SHG microscopy of powder **C14TATP**.